Journal of
Materials Chemistry B

Accepted Manuscript

This article can be cited before page numbers have been issued, to do this please use: J. Chen, L. Li, S. wang, X. Y. Sun, L. xiao, J. Ren, B. Di and N. Gu, *J. Mater. Chem. B*, 2017, DOI: 10.1039/C7TB00864C.

ROYAL SOCIETY OF CHEMISTRY

rsc.li/materials-b

View Article Online
DOI: 10.1039/C7TB00864C

Journal of Materials Chemistry B

ARTICLE

A glucose-activatable trimodal glucometer self-assembled from glucose oxidase and MnO_2 nanosheets for diabetes monitoring

Received 00th January 20xx,
Accepted 00th January 20xx

DOI: 10.1039/x0xx00000x

www.rsc.org/

Jin-Long Chen,*[abc†] Li Li,[ac†] Shuo Wang,[ac] Xiao-Yan Sun,[d] Lu Xiao,[ac] Jia-Shu Ren,[ac] Bin Di,[ac] and Ning Gu*[b]

Daily monitoring of blood glucose is of great importance for the treatment of diabetes mellitus. Herein, we presented an ensemble glucometer with a sandwiched structure formed by the spontaneouse entrapment of glucose oxidase (GOD) onto manganese dioxide nanosheets (MnO_2 NSs) via hydrophobic effect andhydrogen bond interaction. Among of hybrid glucometer, the ultrathin MnO_2 NSs acts as an enzyme nanosupport and target-activated signal transduction. A trimodal self-indicating by fluorescence (FL) and UV-absorbance (UV) and magnetic resonance signal (MRS) activation with glucose-specificy provides a multiple signals of response to glucose. Taking account of operational simplicity and convenience even observed by naked-eye, a detection limit low as 0.1 μM was obtained by using of the ensemble glucometer in colorimetric assay, whilst the precision for 11 replicate detection 10 μM glucose was 3.5% (relative standard deviation, RSD). Notably, the value of the Michaelis–Menton constant of GOD of the presented glucometer is estimated to be 0.051 mM, showing an exceptional enhanced enzymatic activity measured by far. The designed glucometer highlighted with high sensitivity and simplicity was capable of routine blood glucose monitoring for type I diabetes mellitus of rats. Furthermore, the fully integrated platform is readily generalized in principle for a number of biomarkers for point of care diagnostic in the future.

Introduction

The continuous point of care testing of biomarkers gives unique solutions for the treatment of chronic, homeostasis-related diseases such as diabetes mellitus.[1,2] One strategy is the use of multimodal probes response to specific biological species which would help to maximize the signal from the target and minimize background signal, improving sensitivity and specificity.[3,4] Prominent among which is generally developed by integration of signals transduction with active enzymes.[5,6] However, one of the major obstacles for enzyme-involved probes remains the lack of compatible approach for ensemble susceptible native enzymes with signal transduction agents. Recently, two-dimensional nanomaterials have attracted high attention owing to their ultimate structure and fascinating properties. Especially ultrathin MnO_2 NSs with high specific surface area appeared to act as benign cargoes to trap and support drugs and biomolecules which have employed a wide variety of promising applications for stimuli-response drug delivery[7-9] and especially for target-activatable biosensor[4, 10-15] in recent years. However, a powerful platform for biosensing by integrating activatable mediator agents with susceptible enzymes is still challenging free of requirements for either sophisticated instrument and operation or much specific knowledge. Notably, glucose-GOD catalysis cascade reaction as a proof of concept has extensively used in design of biosensors for detection of glucose and many non-glucose targets by far.[16-21] Furthermore, the detection of blood glucose has attracted continuous attention because diabetes mellitus is one of the highest worldwide public health threats. One of the major challenges in the management of these diabetic patients is the frequent monitoring of blood glucose concentrations because good diabetic control is very difficult to achieve.[22, 23] Despite years of research, a variety of methods and techniques have been developed to detect the glucose concentrations, including near-infrared spectroscopy[24, 25], electrochemical biosensors[26] and fluorescence assays[27, 28]. However, most of current methods still require expensive instrumentations and tedious procedures as well as poor selectivity that are not widely available to the general public for quantitative analysis. In contrast, practical glucose monitoring should be accurate, simple, and low cost as far as possible.

We herein presented a glucose-specific response glucometer characterized with readout of multiple signals and high enzymatic activity which was facile obtained just mixing of GOD and MnO_2 NSs in aqueous solution at ambient environment. Significantly different from previous methods and

[a] Department of Pharmaceutical Analysis, School of Pharmacy, China Pharmaceutical University, Nanjing 210009, P. R. China, E-mail: chenjl_4@hotmail.com; Tel: 86-25-83271316; Fax: 86-25-83271316
[b] Jiangsu Key Laboratory for Biomaterials and Devices, School of Biological Science and Medical Engineering, Southeast University, Nanjing, 210096, P. R. China, E-mail: guning@seu.edu.cn; Tel: 86-25-83792576; Fax: 86-25-83794960.
[c] Key Laboratory of Drug Quality Control and Pharmacovigilance (China Pharmaceutical University), Ministry of Education, Nanjing 210009, P. R. China.
[d] Laboratory of Cellular and Molecular Biology, Jiangsu Province Institute of Chinese Medicine, Nanjing 210000, P. R. China
†Jin-Long Chen and Li Li contributed equally to this work.
Electronic Supplementary Information (ESI) available: Experimental materials and methods, characterization data. See DOI: 10.1039/x0xx00000x

View Article Online
DOI: 10.1039/C7TB00864C

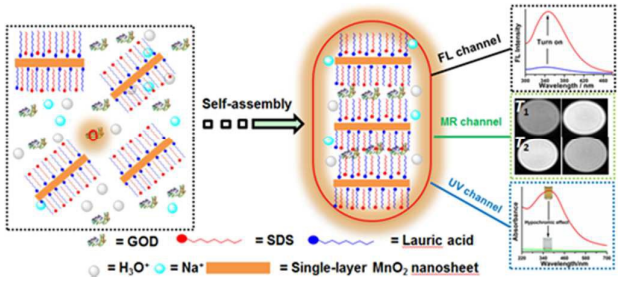

Fig.1 Schematic illumination for an ensemble glucometer with sandwiched structure self-assembled spontaneously from GOD and MnO_2 NSs characterized with an exceptional enhanced enzymatic activity as well as a self-indicating of glucose with readout of three channel signals of UV/MR/FL.

technologies for glucose detection using of GOD and MnO_2 (Fig.1),[4, 10, 13, 15] a self-indicating approach via direct triple signal readout was firstly developed superior to those glucose biosensors with only readout of either single channel or double-channel signals in complex matrixes. Notably, an unusual enhancement of the enzymatic activity of GOD was observed which endowed the ensemble glucometer with high sensitivity favorable for detection of blood glucose especially for colorimetric assay. Furthermore, a diversity of hybrid platforms is readily generalized in principle by integrated MnO_2 with numerous biomolecules for the diagnostics and treatments of diseases in the future.

Experimental section

Materials and Chemicals

H_2O_2 (30%), $KMnO_4$, H_2SO_4, $NaCH_2COOH$ (NaAc), and CH_3COOH (HAc) were purchased from Nanjing Chemical Reagent (Nanjing, China) CO., Ltd. Glucose was purchased from Xilong Chemical. (Guangdong, China). Glucose oxidase from Aspergillus niger (GOD,10KU) was purchased from Aladdin and stored in a refrigerator at -20 ℃. Sodium dodecyl sulfate (SDS) was purchased from SunShineBio company (Nanjing China). Streptozotocin (98%, Sigma, Chemical Co., St. Louis, MO, USA). Humulin 70/30 recombinant human insulin mixed injection (300 u/3 mL, Lilly Suzhou Pharmaceutical Co, China). Fructose, lactose, maltose was purchased from Aladdin. Various amino acids were acquired from Sinopharm Chemical Reagent CO., Ltd. Albumin human (HSA) was purchased from Sigma-Aldrich. All serum samples were collected from type-1 diabetes mellitus SD rat induction by streptozotocin. All other chemicals were of analytical reagent grade and used without further purification. Ultrapure Water (18.2MΩ·cm) was used throughout.

Apparatus

All absorption spectra were measured on a UV-1800 spectrophotometer (Shimadzu, Japan) equipped with a plotter unit and a quartz cell (1 cm × 1 cm), kinetic experiments and scan spectrum. Fluorescence spectra measurement was performed on a Hitachi-F-4600 spectrofluorometer (Tokyo, Japan). T_1- and T_2-weighted MRI images of a certain amount of MnO_2 NSs in different concentrations of H_2O_2, and GOD-MnO_2 NSs in various concentrations of glucose were acquired from a 0.5 T MR scanner (MesoMR60, Shanghai Niumag Corporation, China). The test parameters were as follow: multi spin-echo, TR/TE =2000/60 ms, slices=1, matrix of 192×256 and FOV of 100×100 mm.

The morphology and microstructure of the MnO_2 NSs were characterized by transmission electron microscope (TEM) on a Tecnai G2 F20 (Philips, Holland) operating at 200 kV accelerating voltage. The height profile of MnO_2 NSs was studied by atomic force microscopy (AFM) (Multimode Nanoscope IIIa controller) under tapping mode on a mica substrate. Fourier transform infrared (FT-IR) spectra were measured from a KBr window on a FT/IR-4100 JASCD spectrophotometer. Circular dichroism (CD) spectra were recorded with a J-810 (JASCD). Inductively coupled plasma optical emission spectrometry (ICP-OES) Optima 5300DV was used to analysis concentration of MnO_2 NSs as manganese ion. Commercially available blood glucose meter (GA-3, SANNUO) was applied to detect of blood glucose collected from SD rats.

Preparation of MnO_2 NSs with the assistant of SDS

Colloidal MnO_2 nanosheets were synthesized by one-step with the assistant of SDS in a aqueous acidic solution according to a modified method.[29] Briefly, a diluted H_2SO_4 solution (1.8 M,45 μL) and SDS (461.4 mg) were sequentially added into 160 mL distilled water and heated at 95℃ for 15 min by first, as followings, the temperature of the mixture solution was reduced to 85 ℃. $KMnO_4$ solution (0.05 M,1.6 mL) was rapidly add to the above SDS solution and started to reaction under stirring at 85 ℃ for about 35 min to obtain a dark brown homogeneous solution (Fig. S1). In the formation of water-dispersed single-layer MnO_2NSs, SDS plays as both the precursor of the reductant and a structure-directing agent. As illustrated in Fig.S2, SDS undergoes partially hydrolysis to produce dodecanol in acidic solution which was self-assembled with SDS into a lamellar structure. Subsequently, a redox reaction in situ occurs between dodecanol and $KMnO_4$ to yield lauric acid and MnO_2. Thus, well water-soluble MnO_2 NSs were co-modified with lauric acid and SDS attributing to the coordination interactions of carboxyl group and unsaturated Mn atoms and hydrophobic effect. The synthesized MnO_2 NSs were purified by centrifugation and repeated wash with ultrapure water and ethanol. The purified MnO_2 NSs after freezer-dry was readily suspended in ultrapure water to form a colloidal suspension, which was then dried on corresponding substrates overnight at room temperature for the morphology characterizations of TEM, AFM. For other material characterizations, such as FT-IR and ICP-OES measurements, bulk nanosheets dried from a concentrated solution without substrate were used.

Procedures for detection of glucose by using the presented glucometer in trimodal signals: UV absorption spectroscopy and MRS and fluorescence spectroscopy

Due to hydrophobic effect and hydrogen bond interactions, GOD molecules would be spontaneously entrapped on the surface of MnO_2 NSs via noncovalent approach. An ensemble

View Article Online
DOI: 10.1039/C7TB00864C

glucometer was facile obtained by directly mixing of certain amounts of GOD and MnO_2 NSs in aqueous solution standing at ambient environment for five minutes. A series of considerable aliquot of the ensemble glucometer was added into a set of 5 mL calibrated text tubes on demand of the designated measurements, 1mL of 10 mM NaAc-HAc (pH 5.6) buffer solution and a series of glucose solutions were added in turn. The final mixtures were then diluted to volume with ultrapure water, and mixed thoroughly. Prior to measurements, the mixture solution was incubated in a water bath at 37 ^{0}C for 30 min. Then, the mixture was taken out from the water bath and allowed to cool to room temperature for 5 min for measurements.

Serum samples collection from type-1 diabetes mellitus rat

Streptozotocin (STZ)-induced diabetes mellitus offers a very cost-effective and expeditious technique that can be extensively used in most strains of rodents.[30] Ten adult male SD rats weighed between 200 - 250 g were housed in wire mesh cages at room temperature. Veterinary care was provided by local laboratory animal house unit in Faculty of Medicine, China Pharmaceutical University. All animals were handled according to the guidelines established by institutional animal care and use committees. The rats were divided into two groups (five for one group). All rats were firstly injected intraperitoneally with a single dose of 60 mg/kg of streptozotocin dissolved in sodium citrate buffer (0.1 mol L^{-1}, pH was adjusted to 4.5) at a concentration of 10 mg/ml immediately before use. After 3 days, fasting blood samples were collected through the retro-orbital route using capillary tubes to assess glucose level by using a commercially available glucometer. Animals showing blood glucose higher than 16.7 mM were considered as diabetic and two of them were chosen to use throughout for the study. One of diabetic rats was as followings treated with a 3U of insulin. Changes of serum glucose in different level of type-1 diabetes mellitus induction with streptozotocin coupled with insulin treatment were monitored in a fixed time interval. All serum samples were collected by remove of the clot of whole blood samples under certification that were initially withdrawn from SD rats through retro-orbital route using capillary tubes. All serum samples were subjected to an appropriate dilution before analysis and no other pretreatments were necessary.

Procedures for colorimetric assay by using the presented glucometer for detection of serum glucose

In view of simplicity and convenience, exploration of the ensemble glucometer composed of certain amounts of GOD and MnO_2 NSs for daily blood glucose monitoring by only using of absorption spectroscopy. To a series of 5 mL calibrated test tubes a designated glucometer composed of 1.5 μg mL^{-1} GOD and 35 μM MnO_2 NSs, 1 mL of 10 mM NaAc-HAc (pH 5.60) buffer solution, a serum sample (appropriate for 5.0 μL) or different amounts of standard glucose solution were sequentially added. The mixture solution was mixed thoroughly before addition of a new solution. Prior to spectroscopic measurement，the final mixture solution was incubated in a water bath at 37 ^{0}C for 30 min. Then，the mixture was taken out from the water bath and allowed to cool to room temperature for 5 min for spectroscopic measurements at 374 nm.

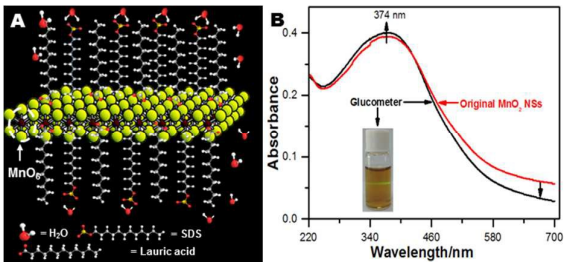

Fig.2 A structural illumination of the synthetic MnO_2 NSs in aqueous solution (A), the representative absorption spectra for free MnO_2 NSs, and the proposed glucometer (B) (inset: photograph for glucometer aqueous solution with Tyndall scattering light).

State:

We will conscientiously abide by the ethical principles of animal welfare, accept the supervision and inspection of the committee of China Pharmaceutical University at any time, and voluntarily accept the punishment if any infringement.

Results and discussion

Design and characterization of the ensemble glucometer

Benefited from ultimate structure and fascinating optomagnetic properties of MnO_2,[31-34] we herein presented an ensemble glucometer with a sandwiched structure programmable enginerred by self-assembly of GOD and MnO_2 NSs in aqueous solution as shown in Fig. 1. Ultrathin MnO_2 NSs with high specific surface area appeared to act as benign hosts to trap and support GOD and signal-transduction moeity with target-activiation. The designed glucometer gave a self-indicating approach of direct readout triple signals of UV/MR/FL simultaneously triggered by an cascade enzymatic reaction. In this study, homogenous dispersion of MnO_2 NSs co-functionalized with lauric acid molecules and SDS (Fig. 2A and Fig. S2 in ESI) was readily obtained by a redox reaction according to a modified literature.[29] The as-obtained MnO_2 NSs was characterized with a broad absorption band from 220 to 700 nm orignating from d-d transition of Mn atoms with a considerable molar extinction coefficiency ($\varepsilon_{374\ nm}$ = 9.0 × 10^3 $M^{-1}cm^{-1}$) (Fig. 2B and Fig S3 in ESI).[34] Compared to free MnO_2 NSs, the ensemble glucometer showed no obvious changes in absorption profile, only a slight decrease of absorbance beyond 450 nm propably due to better dispersion of nanosheets in aqueous solution with aid of GOD. A typical low and high magnification TEM mage of free GOD, as presented in Fig. 3A, indicates a monodispersed similar spherical morphology with a meaning size of 1.8 nm as well as a meaning height approximately of 1.32 nm was identified by respresentative AFM(Fig.3 B-D) greatly smaller than the size of stretch GOD in water solution (Fig. S4A). The as-obtained MnO_2 NSs display transparent lamellar morphologies with lateral sizes estimated to be ~200 nm with a meaning height approximately 0.95 nm between 0.83 nm and 1.16 nm expected

View Article Online
DOI: 10.1039/C7TB00864C

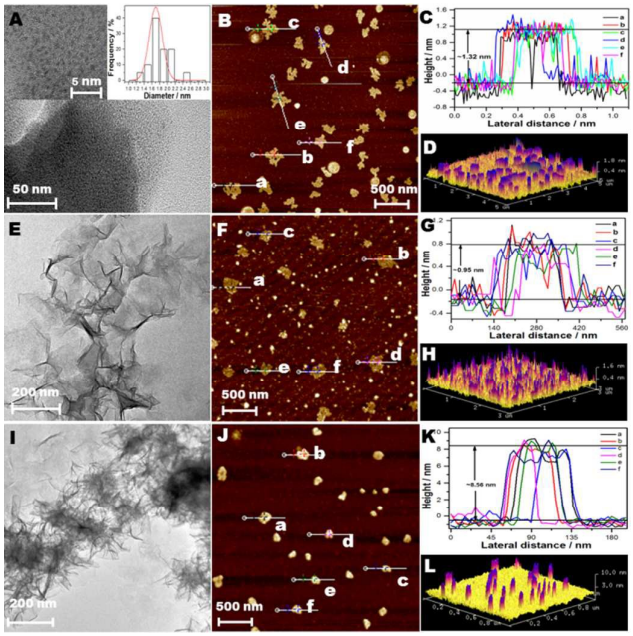

Fig.3 Representative TEM images for free GOD (A) (Inset: HR-TEM image and diameter distribution GOD), MnO_2 NSs (E) and MnO_2 NS-GOD hybrid as the glucometer (I), Tapping-mode AFM 2D and 3D images for free GOD (B, D), free MnO_2 NSs (F, H) and MnO_2 NS-GOD hybrid as the glucometer (J, L) with corresponding height profiles (C,G,K) of six samples marked with lower-case letters from a to f.

for the thickness of single-layer MnO_2 NSs one-side and two-side co-modified with lauric acid and SDS molecules (Fig. S4B) confirmed by TEM (Fig.3E) and AFM (Fig. 3F and H) analysises. Notably, more ample wrinkles and folds were observed for the ensemble glucometer with a cluster-like morphology (Fig. 3I, J) and a significant increase in meaning height to 8.56 nm (Fig. 3K, L) refered to free GOD and MnO_2 NSs, respectively. The height of hierarchical glucometer between 7.76 nm and 10.03 nm is responsible for 3-folds and 4-folds of the sandwiched structure by a full-packed single molecular layer of GOD into double flakes of MnO_2 NSs. Thus, a multiple sandwiched structure of the ensemble glucometer was implied to be spontaneously formed from GOD and MnO_2 NSs via multiple noncovalent interactions as shown in Fig.1.

Self-indicating of glucose using the ensemble glucomter by UV/FL/MR signals

Differ remarkably from MnO_2 NS based either single channel or multimodal sensors as previous reported, a self-indicating approach was developed just by direct readout of intrinsic signals of the individual units of the ensemble glucometer. The presented glucometer was inspired by combination of unique reactivity of MnO_2 (Fig.S5 in ESI) and enzymatic performances of GOD. D-glucose as a substance was catalyzed specifically by GOD into gluconic acid and H_2O_2 described as equation. 1.[35]

$$\beta\text{-D-}C_6H_{12}O_6 + O_2 + H_2O \xrightarrow{\text{GOD}} H_2O_2 + H^+ + C_6H_{11}O_7^- \quad (1)$$

$$MnO_2 + H_2O_2 + 2H^+ \longrightarrow Mn^{2+} + O_2 + 2H_2O \quad (2)$$

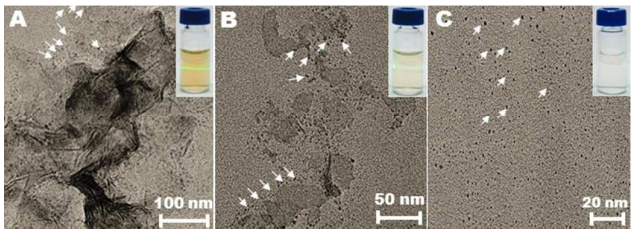

Fig.4 Representative TEM images of the designated glucometer containing of 1.5 μg mL^{-1} GOD and 35 μM MnO_2 NSs upon addition of 20 μM (A), 50 μM (B) and 100 μM (C) glucose (Inset: photographs of the corresponding solutions with Tyndall scattering light, smaller-sized nanoparticles etched by H_2O_2-generated by glucose-GOD catalytic reaction marked with white arrows).

MnO_2 NSs was effective decompsed by H_2O_2 generated from glucose-specfic biocatalytic reaction described above. As seen from Fig. 4A-C, glucose-cascade induced decomposition of the designated glucometer was further justified by TEM images, indicating that MnO_2 NSs was gradually etched into smaller-sized nanofragments starting from nanosheets edge and further soluble Mn^{2+} ions[15] with significant dispearance of its color and Tydall scatterring light. Once MnO_2 NSs are dissolved, the collective changes in absorbance, MRS and fluorescence of the presented glucometer would be observed. Taking in account of temperature and pH effect on GOD activity and H_2O_2-decomposition MnO_2 NSs reaction, the optimization conditions of pH 5.60, 37℃ and 30 minutes were recommended to be used for detection of glucose throughout (Fig. S6 in ESI). As a colorimetric assay (Fig. 5A, B), the absorbance of the ensemble glucometer solution gradually decreased as the concentration of glucose increased, even observed by a naked-eye change in color. The decreased absorbance (ΔA) linearly increased with glucose concentration from 1 μM to 50 μM with a calibration function of $\Delta A = 0.00485[\text{glucose}] + 0.0188$ (R^2=0.992). The limit of detecting of (LOD) (3s) of the present GOD-MnO_2 NSs based nanosesor was 0.1 μM, whilst the precision of for 11 replicate detection 10 μM glucose was 3.5% (relative standard deviation, RSD).

Wherein manganese ions in original MnO_2 NSs modified with long alkyl chain of SDS and lauric acid was shielded from aqueous environment (Fig.2A) , making no contribution to the protons' longitudinal or transverse relaxation. Once Mn^{2+} ions released by decomposition of MnO_2 exhibited greatly changes in both T_1- and T_2 weighted MR signals compared to original MnO_2 NSs.[4, 7, 36]Magnetic nanosensors underlying the princple of OFF/ON or activatable magnetic resonance signals have been designed to identify and quantify a wide variety of target analytes.[37-39] The visualization changes in T_1- and T_2 weighted MR images for the presented glucometer was found in the presence of different amount of glucose (Fig.5C). Plots of the corresponding T_1- and T_2- weighted MR signals intensity difference versus gluocose conctrations displayed a similar relationship From 10 μM to 800 μM (Fig.5D and E).

The intrintic UV fluorescence of GOD was significantly suppressed by MnO_2 NSs through energy transfer or both inner filter efffect process (Fig.S7 in ESI).[11, 40]The caged fluorescence could be lighted up again owing to the gradual

View Article Online
DOI: 10.1039/C7TB00864C

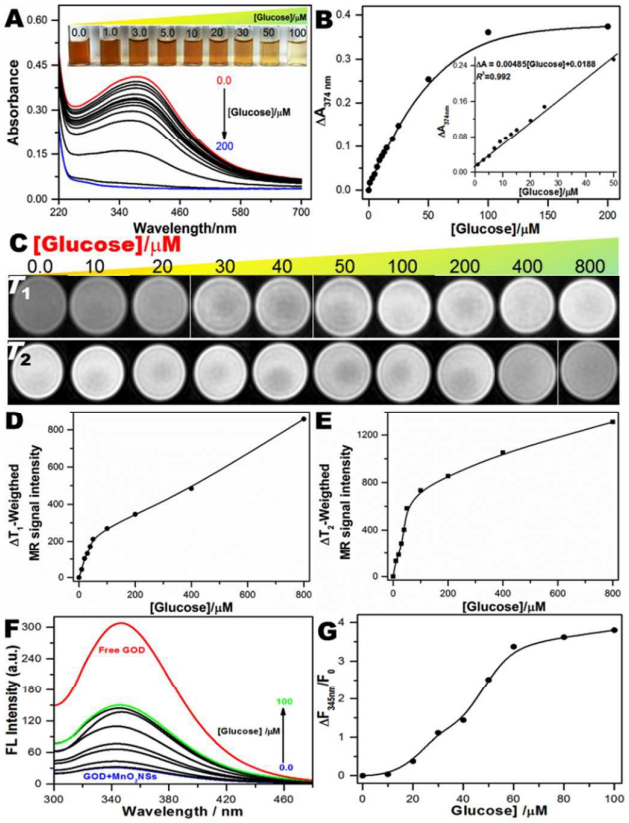

Fig.5 (A) The absorption spectra of the ensemble glucometer at varied glucose solutions in pH 5.6 of 10 mM HAc-NaAc buffer (Inset: photographs of the glucometer solution by addition of a series concentrations of glucose); (B) Plots of the decreased absorbance as function of glucose concentration. (C) T_1-and T_2-weighted MR imaging of the glucometer solutions containing of 5.0 μg mL^{-1} GOD-100 μM MnO_2 NSs at varied concentrations of glucose; Plots of changes on T_1- (D) and T_2-(E) weighted MR signals intensity as a function of glucose concentrations. (F) Fluorescence spectra of free 20 μg mL^{-1}GOD, the ensemble glucometer solutions containing of 20 μg mL^{-1} GOD-150 μM MnO_2 NSs at varied concentrations of glucose, and (G) plot of corresponding $\Delta F_{345\ nm}/F_0$ as a function of glucose concentrations.

decomposition of MnO_2 NSs by H_2O_2 generated from glucose-GOD biocatalytic reaction described above (Fig.5F). Plots of the fluorescence intensity difference of glucometer ($\Delta F_{345nm}/F_0$) versus gluocose concentrations gave a dose-dependent response from 10.0 μM to 100 μM.

With respect to sensitivity and linearable response to glucose, the colorimetric assay using the presented glucometer was particularly favorable in point of care testing free of requirements for either sophisticated instrument or much specific knowledge for luminescence and magnetism.[17, 41]

Mechanism on the enzymatic activity of GOD self-assembled MnO_2 NSs

The enzymatic activity of immobilized enzymes gave an extremely important effect of on the preformances of the ensemble sensing system. To be our well-known that the Michaelis-Menton parameters (K_m and V_{max}) are generally used to evaluate enzyme activity. The parameters were quantitatively estimated by use of the Linweaver-Burke plot as[42]:

$$\frac{1}{v} = \frac{K_m}{V_{max}}\frac{1}{[S]} + \frac{1}{V_{max}} \quad (3)$$

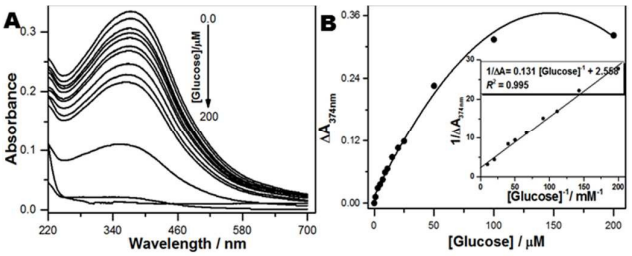

Fig. 6 (A) The absorption spectra of the presented glucometer containing of 1.5 μg mL^{-1} GOD-32 μM MnO_2 NSs in various concentration of glucose (B) Plots of changes at absorbance at 374 nm (ΔA_{374nm} = A-A_0) against glucose concentrations (Inset: Lineweaver-Burke plots of the GOD-glucose reaction.)

Because GOD can specifically catalyze the oxidation of glucose to quantitative production of H_2O_2, it is expected that for a given enzymatic activity, the rate of H_2O_2 production increase with the glucose concentration. In view of H_2O_2-induced decomposition of MnO_2 NSs, the absorbance decrease actually embodies the changes of GOD enzymatic activity. Seen from Fig. 6, the absorbance changes increases with the increasing glucose concentration up to 100 μM, after which it reaches saturation. Thus, a 0.051 mM of K_m was calculated according to the equation described-above as shown in Fig. 6B. It is exceptional 110 folds improvement of enzymatic activity over free GOD with a K_m of 5.85 mM which is greatly lower than that of either covalent conjugation with gold NPs, Fe_3O_4 NPs, Mn-doped ZnS QDs or noncovalent immobilized on ZrO_2/chitosan, ZnO nanorods, graphene as far (Table S1 in ESI). The enzymatic activity is generally acknowledged to be directly related with its second and tertiary structures which are substantial dependent on the interactions between enzymes and as-immobilized supports.[19, 20, 42] FT-IR data showed that the overall absorption profile of the presented glucometer was just a superimposition of MnO_2 NSs and GOD without new absorption band and shift of band (Fig.S8 in ESI). Furthermore, a zeta potential of initial MnO_2 NSs with -24.5 mV changed to -26.2 mV by addition of negative charged GOD in the pH of 5.6 buffer solutions (isoelectronic point of GOD being 4.2). The FT-IR and zeta potential results suggested that a nonconvalent interacation occurred to the process of self-assembly of GOD and MnO_2 NSs via hydrogen bond and hydrophobic effect.

The conformational changes of GOD induced by MnO_2 NSs were systematically investigated by CD spectroscopy, and synchronous fluorescence spectroscopy and electrochemistry test. CD spectroscopy results demonstrated that CD spectrum of free GOD has characteristic peaks at λ = 210 nm and 219 nm, which are retained in the native conformation. Whereas, GOD immobilized by MnO_2 NSs gave new peaks at 208 nm and 216 nm, respectively demonstrating that the precise enzymatic conformation, including α-helix, β-sheet, β-turn, and random coil, changes greatly by contrast to the free GOD (Fig. 7A and Table S2 in ESI). The conformational changes implied a

View Article Online
DOI: 10.1039/C7TB00864C

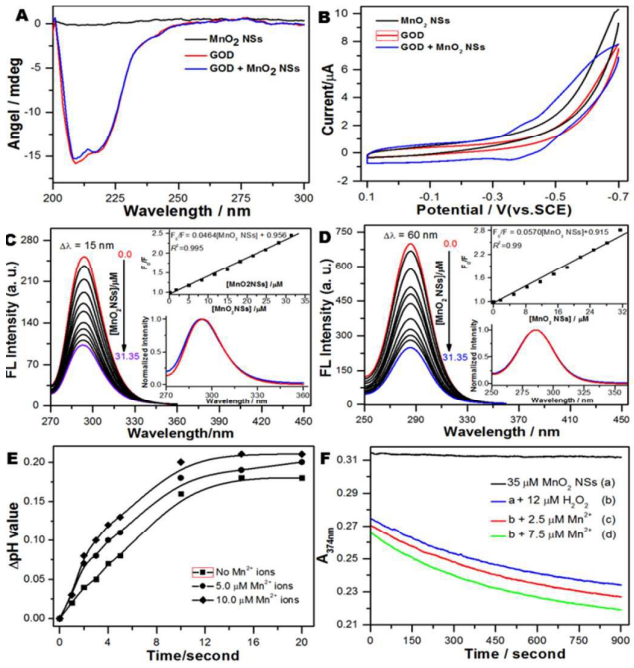

Fig.7 (A) CD spectra of 30 μg mL^{-1} free GOD (red line), 30 μM MnO_2 NSs (black line) and their mixture (blue line), respectively. All samples were dissolved in HAc-NaAc (10 mM, pH 5.6) (B) cyclic voltammetry of MnO_2 NSs|GCE (black line) GOD|GCE (red line) and GOD–MnO_2 NSs|GCE (blue line) in N_2-saturated PBS 0.1 M with a pH 5.6 and scan rate of 100 mV s^{-1}. The synchronous fluorescence (Δλ = 15 nm) (C) and (Δλ = 60 nm) (D) spectra of 20 μg mL^{-1} GOD at varied concentration of MnO_2 NSs (Inset: plots of F_0/F as a function of MnO_2 NSs concentration and Normalized fluorescence profiles of GOD before and after addition of MnO_2 NSs);(E) Effect of trace Mn^{2+} ions on the pH changes of 1.5 μg mL^{-1} GOD-0.12 mM glucose system containing of 2.0 mM KCl from an identical pH of 5.65 (F) Effect of Mn^{2+} ions on 12 μM H_2O_2-induced decomposition of 35 μM MnO_2 NSs.

favorable configuration of GOD with a higher affinity to glucose, resulting to an improvement of enzymatic activity. The direct electrochemistry of GOD using cyclic voltammetry technology, a pair of quasi-reversible redox peaks was only observed at GOD-MnO_2 NSs|GCE (glassy carbon electrode) with the formal peak potentials -0.354 V and peak-to-peak separation (ΔE_p) 32 mV assigned to a charateristic electron transfer of FAD (Fig. 7B) to electrode primary attributing to partial exposure of enzyme active center.[43] The conformational changes were further be identified by fluorescence spectroscopy.[44]

The synchronous fluorescence of GOD was characteristically collected by $\Delta\lambda = 15$ nm and $\Delta\lambda = 60$ nm, assigned to aromatic tyrosine and tryptophan residues which were important for the correct orientation of the substrate as well as for the maximal velocity of glucose oxidation. Concentration of MnO_2 NSs dependent fluorescence of GOD was well followed a Stern-Volmer equation 4:

$$F_0/F = 1 + K_{sv}[MnO_2NSs] \quad (4)$$

Wherein a larger quenching constant (K_{sv}) was obtained for tryptophan residue over tyrosine one that suggested interactions between MnO_2 NSs and GOD was closer to tryptophan residue (Fig.7C and D). Additionally, a slight blue-shift of characteristic synchronous fluorescence originating from tyrosine residue demonstrated transfer tyrosine residues to a more hydrophobic environment accompanied with the partial exposure of of FAD as a redox active center of GOD.

In view of reaction equilibrium theory, rectants in cycles on-demand between GOD-glucose catalytic reaction and H_2O_2-induced decompsition of MnO_2 NSs undoubtedly promotes the decomposition of MnO_2 NSs (Equations 1 and 2) which is favorable for the whole reaction system essential relavant to improvement of enzymatic activity. Last but not least that effect of trace Mn^{2+} ions released from MnO_2 NSs both on GOD activity and H_2O_2-induced decomposition of MnO_2 was related with absorbance changes of MnO_2 NSs. According to Equation 1 for glucose-GOD catalytic oxidation, the activity of GOD also could be directly monitored of pH value changes owing to a production of gluconic acid.[45] Cofactor effect of self-generating of Mn^{2+} ions on the improvement of enzymatic activity of GOD was confirmed by a much faster and larger change of pH of glucose-GOD system at the identical initial pH of 5.65 similar to DNAzyme (Fig. 7E).[8] Furthermore, trace Mn^{2+} ions also gave an stimulation effect on H_2O_2-induced decomposition of MnO_2 NSs indicating by characteristic absorbance evaluation with time, probably originating from Fenton chemistry (Fig. 7F).[46]

In a word, comprehensive enhancement enzymatic activity of GOD with MnO_2 NSs of the ensemble glucometer with favorable configuration of GOD coupled with the partial exposure of active center, on-demand cyclic processes and self-generating manganese (II) ions synergistic catalysis effects including afforded a unusual enhancement of the enzymatic activity of GOD of the ensemble glucometer.

Glucose-specificity and recycling response of the designed glucometer

The target-specific and recycle of the designated glucometer is of great significance for point of care diagnostic analysis. To access the selectivity of the proposed ensemble glucometer composed of GOD-MnO_2 NSs, we tested the influence of conventional relevant metal ions, anions and other molecules in biological fluids on the detection of glucose (50 μM). Remarkably, as shown in Fig. 8, no obvious absorbance changes were observed typical metal ions and anions, amino acids and protein. Furthermore, those potential physiologically substances showed negligible effects on the signal for glucose sensing. Taking advantage of substance-specificity of GOD, several glucose analogues, including maltose, lactose and fructose gave little effect on glucose detection even at its concentrations 6 times higher than that of glucose. Furthermore, considering natural levels of glucose in human blood serum (4.4 to 6.6 mM), while the working range of the proposed method is in the micromolar range with a LOD low to 0.1 μM, relative weak UV absorption signal of blood samples could be largely eliminated only by facile dilution (Fig.S9 in ESI). Thus, the proposed glucometer would work well with small amounts of serum samples, and physiologically relevant interferences as well as matrix effect can be simply eliminated by direct dilution. Notably, the recycle use of the ensemble glucometer is essential

View Article Online
DOI: 10.1039/C7TB00864C

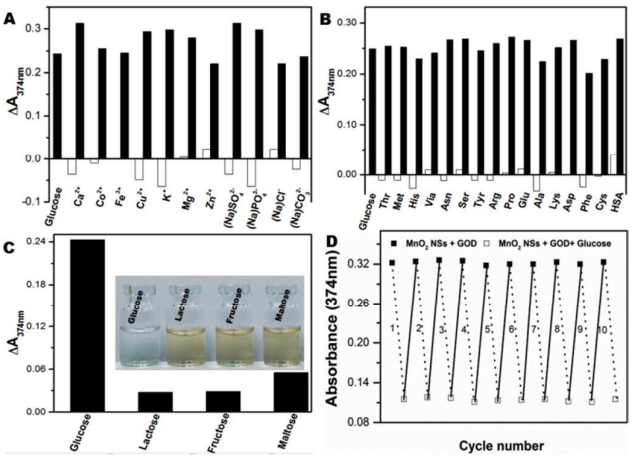

Fig.8 The designated glucometer based colorimetric system response towards various metal cation ions and anions (A), various amino acids and protein (B). The white bars represent the addition of an excess of metal cation ions and anions, various amino acids and protein; The black bars represent the subsequent addition of 50 mM glucose to the corresponding solution described-above (1 mM for K^+, Zn^{2+}, Ca^{2+} and Mg^{2+} and other anions; 0.5 mM for Fe^{3+}) and traditional sugar analogues (C) Inset: the color change with the corresponding solutions.) (D) The absorbance changes of the presented glucometer containing of MnO_2 NSs with successively added in series and GOD in the presence of an identical glucose of 50 μM.

for clinic diagnosis in view of cost-effective. To evaluate the cycle use of the designed glucometer constructed by noncovalent immobilization, a series of identical amount of MnO_2 NSs was successive added to a solution of containing of a fixed GOD of 0.15 μg mL^{-1} in HAc-NaAc (1 mM, pH 5.6). In Fig.8D, similar changes at characteristics absorbance at 374 nm of the presented glucometer were observed after addition of 50 μM glucose. The ensemble glucometer characterized with target-specificity and recycle recognition allows it to accurate quantitative detect of glucose in *in vitro* diagnosis.

Colorimetric assay for routine blood glucose monitoring by using of the presented glucometer

To validate the applicative potential of the hybrid glucometer for routine blood glucose monitoring by only utilize of absorption spectroscopy with respect to simplicity and convenience, we performed daily serum glucose assay of two representative rats chosen from type-1 diabetes mellitus induction by injected intraperitoneally with a dose of 60 mg/Kg streptozotocin. All serum samples were collected by remove of the clot of whole blood samples that were initially withdrawn from SD rats through retro-orbital route using capillary tubes. No additional pretreatments of the serum samples except simple dilution were employed for glucose detection by using the designated glucometer. Shown in Fig.9, a well agreement in the results of serum glucose in various levels was obtained by two methods described-above, displaying the accuracy of the designated glucometer for glucose monitoring. A rat showing continuous and stable blood glucose higher than 16.7 mM was considered as diabetic (Fig. 9A). Insulin-treated diabetics during a 24-hour period showed a significant decrease of blood glucose to normal level while subsequent to an increase to

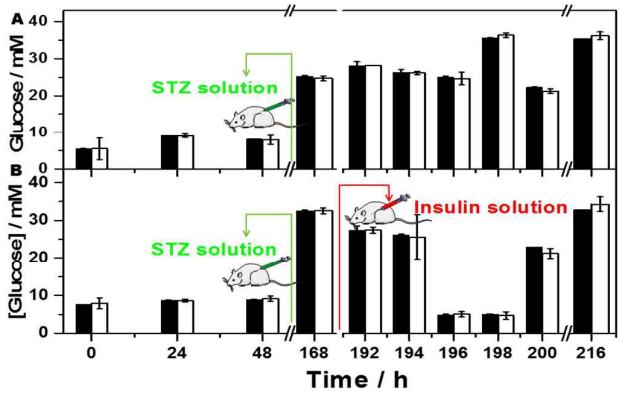

Fig. 9 Blood glucose measurements at a fixed time interval of two representative SD rats of type 1 diabetes mellitus before and after treatment of insulin by using of the presented glucometer (white column) and commercially available blood glucose meter (black column).

diabetic level again resulting from irreversible beta cell destruction (Fig. 9B).[47]

Conclusions

In conclusion, we report that a versatile glucometer was designed by self-assembly of GOD and MnO_2 NSs via noncovalent interactions. Taking advantages of glucose oxidase specificity and unique reactivity of MnO_2 nanosheets, a self-indicating approach for detection of glucose was realized by direct readout of fluorescence/UV/MR signals free of complicated operations. Comprehensive effects including favorable configuration of GOD, on-demand cyclic processes and self-generating manganese (II) ions synergistic catalysis on the exceptional improvement of enzyme activity afforded the presented glucometer with a high sensitive response to glucose. Especially, a colorimetric assay by using the ensemble glucometer with high sensitivity was preferentially available in routine blood glucose monitoring available for type I diabetes mellitus of rats. Meanwhile, the proposed multimodal nanoprobe is readily generalized in principle for a number of biomarkers for point of care diagnostic.

Acknowledgements

The authors are grateful for financial support from the National Natural Science Foundation of China (Grant No. 21350161) and the Natural Science Founding of Jiangsu Province (Grant No. BK20130643), the Fundamental Research Funds for the Central Universities (Grant No. PT2014YX0045), State Key Laboratory of Medicinal Chemical Biology (Grant No.20130404) and Key Laboratory of Drug Quality Control and Pharcovigilance (Grant No. DQCP2015MS06). Postdoctoral foundation of Jiangsu Province (Grant No. 1402153C).

Notes and references

View Article Online
DOI: 10.1039/C7TB00864C

1. H. Lee, T. K. Choi, Y. B. Lee, H. R. Cho, R. Ghaffari, L. Wang, H. J. Choi, T. D. Chung, N. Lu, T. Hyeon, S. H. Choi and D.-H. Kim, *Nat. Nanotechnol.*, 2016, **11**, 566-572.
2. W. Gao, S. Emaminejad, H. Y. Y. Nyein, S. Challa, K. Chen, A. Peck, H. M. Fahad, H. Ota, H. Shiraki, D. Kiriya, D.-H. Lien, G. A. Brooks, R. W. Davis and A. Javey, *Nature*, 2016, **529**, 509-514.
3. A. Louie, *Chem. Rev.*, 2010, **110**, 3146-3195.
4. Z. Zhao, H. Fan, G. Zhou, H. Bai, H. Liang, R. Wang, X. Zhang and W. Tan, *J. Am. Chem. Soc.*, 2014, **136** 11220-11223.
5. C. Li, P. T. Winnard, T. Takagi, D. Artemov and Z. M. Bhujwalla, *J. Am. Chem. Soc.*, 2006, **128**, 15072-15073.
6. H. Xing, C. L. Zhang, G. Ruan, J. Zhang, K. Hwang and Y. Lu, *Anal. Chem.*, 2016, **88**, 1506-1510.
7. Y. Chen, D. Ye, M. Wu, H. Chen, L. Zhang, J. Shi and L. Wang, *Adv. Mater.*, 2014, **26**, 7019-7026.
8. H. Fan, Z. Zhao, G. Yan, X. Zhang, C. Yang, H. Meng, Z. Chen, H. Liu and W. Tan, *Angew. Chem. Int. Ed.*, 2015, **54**, 4801-4805.
9. H. Fan, G. Yan, Z. Zhao, X. Hu, W. Zhang, H. Liu, X. Fu, T. Fu, X.-B. Zhang and W. Tan, *Angew. Chem. Int. Ed.*, 2016, **55**, 5477-5482.
10. R. Deng, X. Xie, M. Vendrell, Y.-T. Chang and X. Liu, *J. Am. Chem. Soc.*, 2011, **133**, 20168-20171.
11. W. Zhai, C. Wang, P. Yu, Y. Wang and L. Mao, *Anal. Chem.*, 2014, **86**, 12206-12213.
12. X.-L. Zhang, C. Zheng, S.-S. Guo, J. Li, H.-H. Yang and G. Chen, *Anal. Chem.*, 2014, **86**, 3426-3434.
13. Y. Wang, K. Jiang, J. Zhu, L. Zhang and H. Lin, *Chem. Commun.*, 2015, **51**, 12748-12751.
14. Y. Yuan, S. Wu, F. Shu and Z. Liu, *Chem. Commun.*, 2014, **50**, 1095-1097.
15. J. Yuan, Y. Cen, X.-J. Kong, S. Wu, C.-L. Liu, R.-Q. Yu and X. Chu, *ACS Applied Materials & Interfaces*, 2015, **7**, 10548-10555.
16. J. Raba and H. A. Mottola, *Crit. Rev. Anal. Chem.*, 1995, **25**, 1-42.
17. R. de la Rica and M. M. Stevens, *Nat. Nanotechnol.*, 2012, **7**, 821-824.
18. L. Rodríguez-Lorenzo, R. de la Rica, R. A. Álvarez-Puebla, L. M. Liz-Marzán and M. M. Stevens, *Nat. Mater.*, 2012, **11**, 604-607.
19. L. Cao, J. Ye, L. Tong and B. Tang, *Chem. Eur. J.*, 2008, **14**, 9633-9640.
20. P. Wu, Y. He, H.-F. Wang and X.-P. Yan, *Anal. Chem.*, 2010, **82**, 1427-1433.
21. R. Gill, L. Bahshi, R. Freeman and I. Willner, *Angew. Chem. Int. Ed.*, 2008, **47**, 1676-1679.
22. M. Bopp, U. Zellweger and D. Faeh, *Diabetes Care*, 2011, **34**, 2387-2389.
23. J. E. Shaw, R. A. Sicree and P. Z. Zimmet, *Diabetes Res. Clin. Pract.*, 2010, **87**, 4-14.
24. H. M. Heise, R. Marbach, T. Koschinsky and F. A. Gries, *Artif. Organs*, 1994, **18**, 439-447.
25. S. F. Malin, T. L. Ruchti, T. B. Blank, S. N. Thennadil and S. L. Monfre, *Clin. Chem.*, 1999, **45**, 1651-1658.
26. J. Wang, *Chem. Rev.*, 2008, **108**, 814-825.
27. J. C. Pickup, F. Hussain, N. D. Evans, O. J. Rolinski and D. J. S. Birch, *Biosens. Bioelectron.*, 2005, **20**, 2555-2565.
28. X. Wu, Z. Li, X.-X. Chen, J. S. Fossey, T. D. James and Y.-B. Jiang, *Chem. Soc. Rev.*, 2013, **42**, 8032-8048.
29. Z. Liu, K. Xu, H. Sun and S. Yin, *Small*, 2015, **11**, 2182-2191.
30. M. C. Deeds, J. M. Anderson, A. S. Armstrong, D. A. Gastineau, H. J. Hiddinga, A. Jahangir, N. L. Eberhardt and Y. C. Kudva, *Lab. Anim.*, 2011, **45**, 131-140.
31. Y. Hao, L. Wang, B. Zhang, D. Li, D. Meng, J. Shi, H. Zhang, Z. Zhang and Y. Zhang, *Int. J. Nanomed.*, 2016, **11**, 1759-1778.
32. Q. Chen, L. Feng, J. Liu, W. Zhu, Z. Dong, Y. Wu and Z. Liu, *Adv. Mater.*, 2016, **28**, 7129-7136.
33. Y. Omomo, T. Sasaki, Wang and M. Watanabe, *J. Am. Chem. Soc.*, 2003, **125**, 3568-3575.
34. K. Kai, Y. Yoshida, H. Kageyama, G. Saito, T. Ishigaki, Y. Furukawa and J. Kawamata, *J. Am. Chem. Soc.*, 2008, **130**, 15938-15943.
35. S. B. Bankar, M. V. Bule, R. S. Singhal and L. Ananthanarayan, *Biotechnol. Adv.*, 2009, **27**, 489-501.
36. P. Mi, D. Kokuryo, H. Cabral, H. Wu, Y. Terada, T. Saga, I. Aoki, N. Nishiyama and K. Kataoka, *Nat. Nanotechnol.*, 2016, **11**, 724-730.
37. L. Josephson, J. M. Perez and R. Weissleder, *Angew. Chem. Int. Ed.*, 2001, **40**, 3204-3206.
38. M. Zhao, L. Josephson, Y. Tang and R. Weissleder, *Angew. Chem. Int. Ed.*, 2003, **42**, 1375-1378.
39. G. Liang, H. Chen, S. Zhang, W. Wu and J. Kong, *Analyst*, 2012, **137**, 675-679.
40. J. F. Sierra, J. Galbán and J. R. Castillo, *Anal. Chem.*, 1997, **69**, 1471-1476.
41. Y. Jiang, H. Zhao, Y. Lin, N. Zhu, Y. Ma and L. Mao, *Angewandte Chemie*, 2010, **122**, 4910-4914.
42. P. Pandey, S. P. Singh, S. K. Arya, V. Gupta, M. Datta, S. Singh and B. D. Malhotra, *Langmuir*, 2007, **23**, 3333-3337.
43. H.-Z. Zhao, J.-J. Sun, J. Song and Q.-Z. Yang, *Carbon*, 2010, **48**, 1508-1514.
44. S. Weiss, *Science*, 1999, **283**, 1676-1683.
45. Y. Zhang, J. Yang, J. Nie, J. Yang, D. Gao, L. Zhang and J. Li, *Chem. Commun.*, 2016, **52**, 3474-3477.
46. D. T. Sawyer, A. Sobkowiak and T. Matsushita, *Acc. Chem. Res.*, 1996, **29**, 409-416.
47. A. Like and A. Rossini, *Science*, 1976, **193**, 415-417.

View Article Online
DOI: 10.1039/C7TB00864C

Table of content

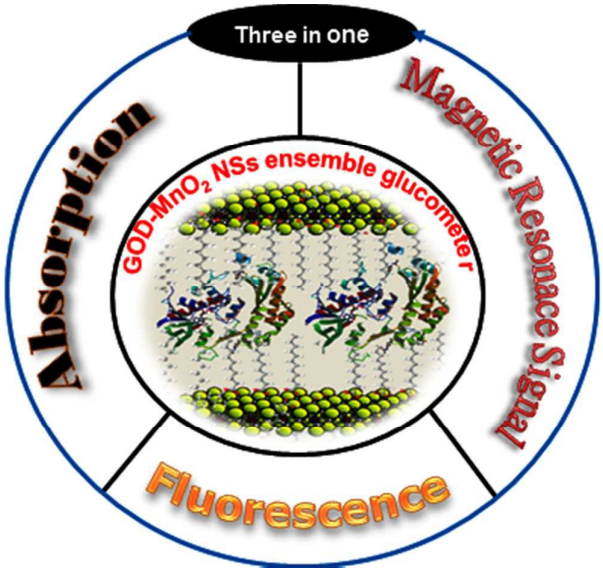

It is the first time to present a glucose-activatable trimodal glucometer with an exceptional enhanced enzymatic activity self-assembled from glucose oxidase and MnO_2 Nanosheets for diabetes monitoring *in vitro.*